

RESEARCH ARTICLE

Dose-dependent proteomic analysis of glioblastoma cancer stem cells upon treatment with γ -secretase inhibitor

Lan Dai¹, Jintang He², Yashu Liu², Jaeman Byun³, Anuradha Vivekanandan³, Subramaniam Pennathur³, Xing Fan^{4*} and David M. Lubman²

¹ Program of Bioinformatics, University of Michigan Medical Center, Ann Arbor, MI, USA

² Department of Surgery, University of Michigan Medical Center, Ann Arbor, MI, USA

³ Department of Internal Medicine, University of Michigan Medical Center, Ann Arbor, MI, USA

⁴ Department of Neurosurgery and Cell and Developmental Biology, University of Michigan Medical Center, Ann Arbor, MI, USA

Notch signaling has been demonstrated to have a central role in glioblastoma (GBM) cancer stem cells (CSCs) and we have demonstrated recently that Notch pathway blockade by γ -secretase inhibitor (GSI) depletes GBM CSCs and prevents tumor propagation both in vitro and in vivo. In order to understand the proteome alterations involved in this transformation, a dose-dependent quantitative mass spectrometry (MS)-based proteomic study has been performed based on the global proteome profiling and a target verification phase where both Immunoassay and a multiple reaction monitoring (MRM) assay are employed. The selection of putative protein candidates for confirmation poses a challenge due to the large number of identifications from the discovery phase. A multilevel filtering strategy together with literature mining is adopted to transmit the most confident candidates along the pipeline. Our results indicate that treating GBM CSCs with GSI induces a phenotype transformation towards non-tumorigenic cells with decreased proliferation and increased differentiation, as well as elevated apoptosis. Suppressed glucose metabolism and attenuated NFR2-mediated oxidative stress response are also suggested from our data, possibly due to their crosstalk with Notch Signaling. Overall, this quantitative proteomic-based dose-dependent work complements our current understanding of the altered signaling events occurring upon the treatment of GSI in GBM CSCs.

Received: November 14, 2011

Revised: August 26, 2011

Accepted: August 31, 2011



Keywords:

Cancer stem cells / Cell Biology / Glioblastoma / Label-free / Multiple reaction monitoring / Pathway analysis

1 Introduction

Glioblastoma multiforme (GBM) is the most aggressive class of brain tumors and 80% of patients with GBM survive

Correspondence: Professor David M. Lubman, Maude T. Lane Professor of Surgery University of Michigan Medical Center, Department of Surgery, 1150 W. Medical Center Drive, MSRB I, A510B, Ann Arbor, MI 48109-0650, USA

E-mail: dmlubman@umich.edu

Fax: +1-734-615-2088

Abbreviations: CSC, cancer stem cell; ENOG, γ -enolase; GBM, glioblastoma multiforme; GFAP, glial fibrillary acidic protein; GSI, γ -secretase inhibitor; IPA, ingenuity pathway analysis; MRM, multiple reaction monitoring; NEST, nestin; PCNA, proliferating cell nuclear antigen; SODC, superoxide dismutase [Cu-Zn]

only for 1–2 years after diagnosis [1]. The emerging evidence for the involvement of brain cancer stem cells (CSCs) in the initiation and propagation of brain tumors, particularly GBM, allows for the identification of more effective therapeutic targets [2]. Several groups have identified brain tumor CSCs using cell surface markers such as CD133 and CD15 [3–5], although currently there is no universally accepted collection of CSC markers for isolation of a pure population of GBM stem cells [6]. GBM neurosphere cultures are often utilized as an alternative to provide an advanced model for investigating GBM CSCs [7].

The importance of Notch signaling in cancer has been firmly established and it is one of the most intensively

*Additional corresponding author: Dr. Xing Fan

E-mail: xingf@umich.edu

studied therapeutic targets in CSCs. Increasing evidence has implicated its central role in GBM [7–10] based on its participation in regulation of self-renewal and cell fate determination in normal stem cells [11]. Therefore, the investigation of the molecular mechanism upon blocking at multiple stages of the Notch signaling cascade become essential where inhibition via γ -secretase inhibitors (GSIs) are the most utilized [6]. We have demonstrated in our previous study that Notch pathway blockade by GSI targets brain tumor CSCs through decreased proliferation and induced differentiation and apoptosis [7, 9, 12].

The conventional biomarker discovery pipeline usually begins with a global unbiased screening stage, which is typically MS-based. A quantitative MS proteomic approach has been demonstrated to be a powerful tool in the study of stem cells utilizing either stable isotope labeling methods or label-free methods [13–16]. To gain further insight into the effects GSI exerts on Notch signaling and other potential pathways involved in GBM CSCs, we have employed a spectral counting-based label-free quantitative proteomic approach to perform a large-scale screening in global discovery phase. This initial profiling provides us comprehensive information about the proteome alterations, which then requires verification after candidate prioritization via a multilevel filtering strategy. Also, the biomarker discovery pipeline usually involves a secondary targeted quantitative stage which traditionally relies on antibody-based protocols such as ELISA to follow up the proteomics or genomic profiling studies [17].

Currently, there has been a trend toward the development of targeted MS as a methodology for confirmation based on the use of multiple reaction monitoring (MRM) [18, 19]. The concept of monitoring specific peptides from proteins of interest as an accurate quantification strategy is well established, because MRM offers superior sensitivity and selectivity for the targeted analytes and the precision is further increased by facilitating the chromatographic retention time as another identifier. Owing to the complementarity of immunoassay and MRM, we have explored a combination of these two assays to verify selected high-priority protein candidates. Moreover, literature mining was performed together with ingenuity pathway analysis (IPA) to relate our findings to previous publications in order to broaden our current knowledge about the underlying molecular mechanisms regarding alterations occurring upon GSI treatment in GBM CSCs. A putative altered signaling network is generated to summarize our findings reflecting those in light of previous publications and those newly mined from our data.

2 Experiments and materials

2.1 Cell culture and treatments

GBM neurosphere cultures were maintained in Neurocult medium (Stem Cell Technologies, Vancouver, BC, Canada,

<http://www.stemcell.com>) supplemented with epidermal growth factor (10 ng/mL) and fibroblast growth factor (10 ng/mL) as previously described [7, 20]. For treatment studies, cells were plated and allowed to grow overnight in Neurocult medium; Neurocult was then replaced the next morning with medium containing γ -secretase inhibitor ([11-endo]-*N*-(5,6,7,8,9,10-hexahydro-6,9-methanobenzo[*a*]8]annulen-11-yl)-thiophene-2-sulfonamide, referred to as “GSI”) [9] dissolved in dimethyl sulfoxide (DMSO) at the concentrations of 0, 2, 10, and 50 μ M. We have shown previously that GSI can block Notch signaling pathway at Hes1 protein expression level starting at 2 μ M level [7, 9].

2.2 Cell lysis and trypsin digestion

Cells were harvested on day three and washed twice with PBS (0.01 M phosphate, 0.15 M NaCl, pH 7.4) to remove culture medium. The extraction of whole cell lysates follows the procedure as previously described [16]. Basically, cell pellets were resuspended in PPS (3-[3-(1,1-bisalkyloxyethyl)pyridin-1-yl]propane-1-sulfonate, Protein Discovery, Knoxville, TN, USA) powder dissolved in 50 mM ammonia bicarbonate at a final concentration of 0.2% m/v together with 1% protease inhibitor cocktail. Protein concentration was determined by Micro BCA™ Protein Assay Kit (Pierce/Thermo Scientific, Rockford, USA). Trypsin digestion, cleavage of PPS, and purification of peptides were performed sequentially and also follow the same protocol [16]. To be noted, PPS is unique among special surfactants for protein solubilization in that it produces no oily film or cloudy pellet in the protein sample solution which may cause protein losses. The degradation of the reagent through acid-cleavage circumvents the major limitation of conventional protein solubilization protocols where detergent suppresses the ionization of low-abundance species. Peptides were then lyophilized to powder and stored in a -80°C freezer for future use. All chemicals were purchased from Sigma unless mentioned otherwise.

2.3 Reversed-phase liquid chromatography and ESI-ion trap mass spectrometry

Peptides were reconstituted in a solution of 5% ACN with 0.1% formic acid at a final concentration of 100 ng/ μ L. Reversed-phase LC was performed by a Paradigm MG4 micropump system (Michrom Biosciences, Auburn, CA, USA) connected to an LTQ mass spectrometer (Thermo Finnigan, San Jose, CA, USA). Total tryptic digests of each sample (control and three treatments) were directly introduced into an RPLC nano-column (3 μ m \times 100 \AA , 0.075 mm \times 150 mm, C18 AQ particles, Michrom) after a desalting nano-trap (300 \times 50 mm) (Michrom). A 3 h linear gradient with 150 min from 5 to

40% ACN, 15 min from 5 to 80% ACN and another 15 min for equilibrium to 5% ACN was used. The other LTQ parameters are the same as previously described [16]. The separated peptides were then introduced into an LTQ equipped with a nano-spray ion source (Thermo Electron). The LTQ was operated in data-dependent mode in which one cycle of experiments consisting of one full MS scan was followed by five pairs of zoom scans and MS/MS scans with dynamic exclusion set to 30 s. The capillary temperature was set at 175°C, spray voltage was 2.8 kV, capillary voltage was 30 V and the normalized collision energy was 35% for fragmentation. Each sample was analyzed in triplicate with each injection of 1 µg material.

2.4 Database searching and multilevel filtering

MS/MS spectra were searched against Uniprot database (updated 05/2010) by SEQUEST search engine incorporated in Proteome Discoverer (version 1.1.0.263). Searching parameters were specified as follows: (i) Fixed modification: carbamidomethylation of Cys residue with a mass shift of 58.1 Da; (ii) variable modification: oxidation of Met residue with a mass shift of 15.99 Da; (iii) two missed cleavage sites were allowed; (iv) peptide ion mass tolerance: 1.4 Da; (v) fragment ion mass tolerance: 1.0 Da; (vi) peptide charges +1, +2, and +3. Searching results were further uploaded to Scaffold (v2.0) as msf format (the default output format from Proteome Discoverer) and global normalization of the spectral counts was performed subsequently. Then, a multilevel filtering strategy consisting of four checkpoints is adopted to capture the most confident identifications and differentially expressed proteins. Checkpoint-1 is based on the FDR test from target-decoy database search with a cutoff p -value < 0.05; Checkpoint-2 is according to the Trans-Proteomic Pipeline (TPP) [21] built in Scaffold. The criteria include protein and peptide probabilities above 95% and a minimum of two unique peptides identified for each protein; Checkpoint-3 is tested by first generating three lists of differentially expressed proteins by applying Student's t -test for 0 versus 2 µM, 0 versus 10 µM and 0 versus 50 µM with a threshold p -value < 0.05 and then retaining proteins that are present in all three lists; Checkpoint-4 is a further filtering based on the literature mining to retain proteins that have been previously reported to play important roles in furthering CSC properties and/or tumorigenesis.

2.5 Western blot

Western blot was performed essentially as previously described [1]. Briefly, 20 µg of total proteins from each sample were separated by 4–20% SDS-PAGE and then transferred to PVDF membranes (Bio-Rad, CA, USA). After

being blocked for 2 h, the membranes were incubated with antibodies including polyclonal anti-APC5, polyclonal anti-GFAP, monoclonal anti-ENGO, monoclonal anti-PCNA, polyclonal anti-SODC and monoclonal anti-Actin (Abcam, Cambridge, CA, USA) overnight. After washing three times, the membranes were incubated with peroxidase conjugated goat anti-rabbit or anti-mouse IgG (H+L) for 1 h. The blots were visualized with DAB stain (Vector Laboratory, WI, USA).

2.6 MRM assays

For the proteins of interest, the selection criteria of proteolytic signature peptides include: (i) being identified from the LTQ analysis with high confidence; (ii) a unique signature of the target protein; (iii) a length of 8–20 amino acids; (iv) no missed cleavage sites; (v) no post translational modifications. Isotope-labeled standard peptides (purity > 98%) were synthesized by Anaspec (Fremont, CA, USA), where the C-terminal lysine or arginine was fully labeled with ¹³C and ¹⁵N. The MRM assay was performed with an Agilent 6410 triple quadrupole MS system equipped with an Agilent 1200 LC (Agilent Technologies, New Castle, DE, USA) in positive-ion mode. Synthetic peptides were first reconstituted in 50% methanol. Flow injection analysis (FIA) was used to optimize the fragmentor voltage and collision energy determined by the intensity of precursor ions and product ions, respectively. Up to four transitions from each peptide were chosen to obtain the best signal-to-noise ratio in MRM mode. A C-18 column from Agilent with 1.8 µm particle size and 4.6 × 50 mm dimension was used for the HPLC separation. The mobile phase is 0.1% formic acid (Solvent A) and 0.1% formic acid in ACN (Solvent B). The linear gradient was 2–20% ACN for 1.5 min and 20–95% ACN for 5 min with a flow rate of 0.6 mL/min. The desolvation gas temperature is 350°C and the capillary voltage is 4000 V. The nebulizer pressure is 45 psi and the desolvation gas flow rate is 11 L/min.

For the monitoring of sample response, three dose (0, 2, and 10 µM) points were interrogated with a total sample protein injection of 10 µg analyzed in duplicates. Data analysis was carried out by Agilent Mass Hunter Quantitative Analysis Software.

2.7 IPA

The three lists of differentially expressed proteins generated after checkpoint-3 were uploaded to IPA together with their fold changes as three different observations. Pathway analysis was then performed to infer the significantly altered pathways associated with GSI treatments. The significance values for analysis of pathway generation were calculated using the right-tailed Fisher's exact t test.

3 Results and discussion

3.1 Protein identifications and differential expression

A 1-D separation strategy was adopted in place of a 2-D approach used in our previous studies [16, 22] by reducing the particle size of the nano-RPLC column from 5 to 3 μm and prolonging the gradient time from 1 h to 3 h to avoid protein losses while also saving instrument time. A total of 1127, 929, 854, and 638 proteins were identified for each sample respectively after filtering by a threshold of $\text{FDR} < 0.05$. Detailed information regarding the identifications for each run can be found in Supporting Information 1. Four Venn diagrams showing the overlap of protein identifications between samples of the same condition were also generated to evaluate sampling reproducibility (Supporting Information 2). For example, the three replicated runs for GSI-0 μM have identified 681, 720, and 725 proteins with 394 shared by all three runs. In order to improve the confidence of protein identifications, a multi-level filtering strategy is employed as shown in Fig. 1. A total of 1707 proteins combining all replicate runs across different samples were identified after checkpoint-1 and a fraction of 672 proteins were retained after checkpoint-2. Next, three lists of differentially expressed proteins were generated for each pair (0 versus 2 μM , 0 versus 10 μM , and 0 versus 50 μM) by a cut-off p -value < 0.05 , resulting in 117, 187, and 213 differentially expressed proteins respectively.

In previous studies, we have already shown that the Notch signaling pathway can be blocked by treating CSCs with 2 μM GSI [7, 9, 12]. The results indicate that the changes of related pathways have occurred at the 2 μM GSI level; however, this was suggested by monitoring the change in one important protein Hes 1 in the Notch pathway. In this study, we investigated the overall protein profiling of GBM stem cells to reveal global proteome changes upon GSI treatment starting at the μM GSI level. Therefore, Student's t -test was applied to choose differentially expressed proteins between GSI-0 μM and 2 μM . Then, we further analyzed the protein changes of GBM stem cells upon treatment of GSI with higher doses (10 and 50 μM). The aim was to discover if the protein changes in Notch signaling and other potential pathways can be intensified by increasing the doses of GSI. Therefore, only proteins exhibiting the same trend of changes under all three concentrations were considered as our candidates. Checkpoint-3 which requires the presence in all three differential expression lists with consistent changing pattern further narrows down the number of putative candidates to 36 (Supporting Information 4).

3.2 Evaluation of label-free quantification

Reproducibility is an essential factor to evaluate the accuracy of a label-free-based quantification approach. It is interrogated from three aspects in this study: variation of the number of protein identifications across three technical

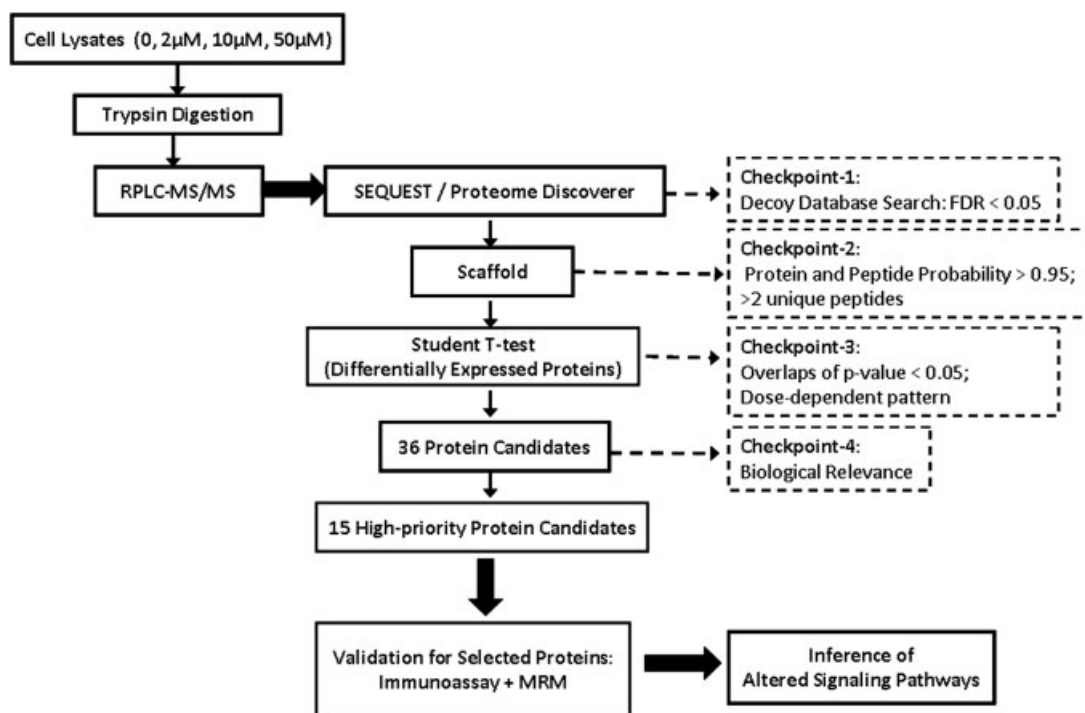


Figure 1. Overall workflow.

replicates; the correlation of spectral counts between any two technical replicates within the same sample and the average variation of all protein identifications based on their spectral counts in between the technical replicates. First, the number of total identifications passing checkpoint-1 in each replicate run is similar to each other with a coefficient of variance (CV) of 3, 1, 3, and 8% for each of the control and 2, 10, 50 μM treatment samples, respectively. Second, high Pearson correlation coefficients are found by comparing any two replicates within the same sample. For example, the coefficient is calculated to be 0.977 between [0.973, 0.982] at 95% confidence level based on the spectral counts assigned to each identified protein between the first and the second technical replicate runs of the control sample. A detailed correlation matrix between all 12 observations across different samples can be found in Supporting Information 3. This correlation matrix was also used to generate the clustering graph shown in Fig. 2. The four different biological entities are clearly separated with their technical replicates grouped under the same branch. Also, the three treatment groups are more closely associated compared with the control group where 2 and 10 μM dose treatments tend to be more closely related compared with the 50 μM treatment. Another way to evaluate the reproducibility is by calculating the average CV (indicated in Supporting Information 2) for all protein identifications across technical replicates. We have observed a consistent $\sim 30\%$ average variation for all four conditions.

3.3 Selection of putative protein candidates

The list of 36 protein candidates were further screened through literature mining to link their biological roles pertaining to CSCs properties and/or dysregulated events in tumors. A total of 15 high-priority putative candidates were

selected as listed in Table 1 and are categorized by different functions: proliferation, differentiation, apoptosis, tumor invasion, oxidative response, and glycolysis. Four proteins (proliferating cell nuclear antigen (PCNA), nestin (NEST), drebrin (DREB), superoxide dismutase [Cu-Zn] (SODC)) from different functional categories in this table were selected for validations by either Western blot or MRM assays. Three proteins out of this table were also selected because of their association with these investigated functions: γ -Enolase (ENOG) (alternatively: neuron-specific enolase (NSE)) for “Proliferation”; glial fibrillary acidic protein (GFAP) for Differentiation; Anaphase-promoting complex5 (APC5) for apoptosis.

3.4 Validation through Western blot

The fold changes of five proteins were validated by Western blot experiments for two dose treatments (2 and 10 μM) of an independent control sample. Figure 3 illustrates a consistent dose-dependent pattern detected between the spectral counting method and Western blot experiments. PCNA is commonly used as a cell proliferation index and a good candidate for prognosis of tumor and cancer development [23]. The decreased expression pattern of PCNA detected in GBM CSCs in our study agrees with a previous report that disruption of Notch signaling by GSI in tracheal epithelial cells reduces PCNA expression [24] and our previous study showing Notch pathway inhibition by GSI reduces CSC proliferation [7, 9]. ENOG has been used as a neuron stem cell marker [25]. A previous study of different subgroups of GBM tumor-initiating cells shows 70% of ENOG-positive cells have developed tumors using a mice xenograft model [26] and the expression of ENOG are only detected in high-grade GBMs [27]. Our finding of down-regulated expression of ENOG may imply that GBM CSCs exhibit a reduced tumor grade as the drug dose increases.

GFAP was chosen to verify the impact of GSI on the differentiation of GBM CSCs. It has been previously detected in $\sim 78\%$ differentiated brain tumor CSCs and exhibits lack of immunoreactivity in undifferentiated CSCs [28]. Our result of up-regulated GFAP expression indicates the treatment of GSI drives GBM CSCs towards a more differentiated state. There is a minor discrepancy between spectral counting and Western blot results when comparing the dose of 2–10 μM . Western results shows the expression of GFAP follows a linear trend as the dose increases while the spectral counting results do not suggest the same. This may be due to the low base expression level of GFAP (spectral counts < 10) where the error bar between technical replicates is comparable to the variation between different conditions. For the verification of altered apoptotic activity upon GSI treatment, APC5 which is a subunit of the multiprotein complex that controls mitotic progression [29] was tested here. It is hypothesized that the abnormal regulation of APC may be involved in malignant transformation

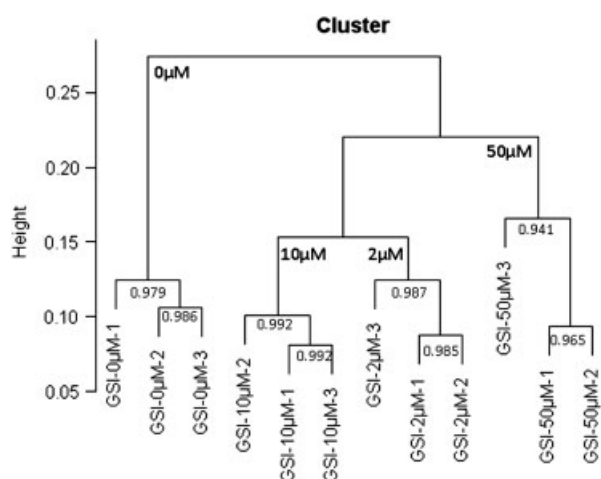


Figure 2. Cluster analysis based on the correlation matrix. Pearson correlation coefficients are shown between technical replicates within the same group.

Table 1. List of high-priority protein candidates after multilevel filtering

Functions	Accession	Protein name	Gene name	p-Value
Proliferation	PCNA_HUMAN	Proliferating cell nuclear antigen	PCNA	0.0016 ↓
	NEST_HUMAN	Nestin	NES	0.0067 ↓
	PA2G4_HUMAN	Proliferation-associated protein 2G4	PA2G4	0.0080 ↓
Differentiation	TBB3_HUMAN	Tubulin β -3 chain	TUBB3	0.0241 ↑
Apoptosis	1433B_HUMAN	14-3-3 Protein β/α	YWHA B	0.0028 ↓
	VDAC1_HUMAN	Voltage-dependent anion-selective channel protein 1	VDAC1	0.0030 ↓
	1433T_HUMAN	14-3-3 protein theta	YWHA Q	0.0053 ↓
	1433F_HUMAN	14-3-3 protein eta	YWHA H	0.0116 ↓
	PDIA1_HUMAN	Protein disulfide-isomerase	P4HB	0.0093 ↓
	TCPB_HUMAN	T-complex protein 1 subunit β	CCT2	0.0128 ↓
	1433E_HUMAN	14-3-3 protein epsilon	YWHA E	0.0139 ↓
Tumor Invasion	DREB_HUMAN	Drebrin	DBN1	0.0043 ↓
	MYH9_HUMAN	Myosin-9	MYH9	0.0191 ↓
Oxidative Response	SODC_HUMAN	Superoxide dismutase [Cu-Zn]	SOD1	0.0238 ↓
Glycolysis	KPYM_HUMAN	Pyruvate kinase isozymes M1/M2	PKM2	0.0186 ↓

p-Value shown here is the average from the three pairs student *t*-tests. ↓ indicates down-regulation of a protein after GSI treatment; ↑ indicates up-regulation of a protein after GSI treatment.

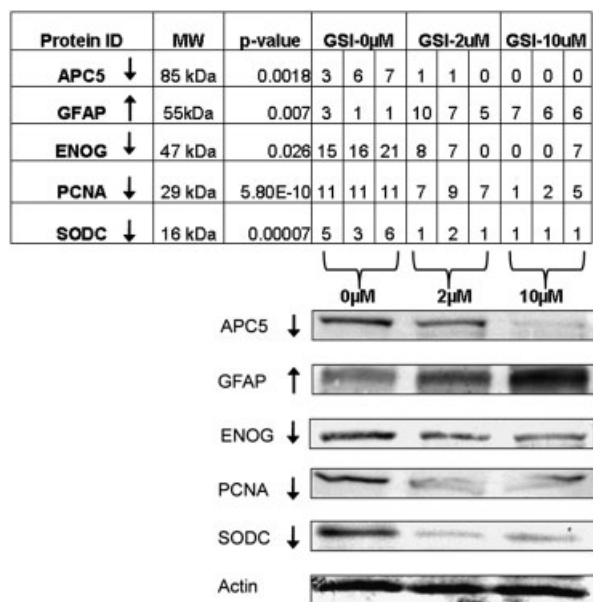


Figure 3. The upper panel shows the spectral counts detected for each protein across replicate runs within each sample. The lower panel shows the corresponding Western blot results. The direction of arrow indicates either up or down-regulated expression.

through chromosome instability [30] and the inhibition may lead to cell death [31]. Thus, our observation of reduced expression level of APC5 may be an indication of cell cycle failure in GBM CSCs after treatment with GSI which in turn promotes cell death. SODC is an important antioxidant enzyme which protects cells from free radical attack and it has been demonstrated to play a critical role in Reactive Oxygen Species (ROS) defense and is associated with chemoresistance and malignancy grade in astrocytic

brain tumors [32]. Thus, the reduced expression level of SODC detected in our experiments may imply that the GSI treatment may render GBM CSCs more vulnerable to apoptosis by attenuating their cell defense system. Overall, the Western blot results of these five proteins suggest three areas of impact on GBM CSCs upon GSI treatment: reduced proliferative potential, increased differentiation, and enhanced apoptotic activity. All of these could be viewed as a decrease of stem cell properties, leading to a phenotype change.

3.5 Validation through MRM

In addition to immunoassay, MRM is also employed as another orthogonal verification strategy to validate the turnover of an important candidate NESTINs in this study. NESTIN has been identified as a neural stem cell marker and a GBM CSC marker [9, 28, 33]. We and others have demonstrated previously that NESTIN expression is enhanced by Notch signaling in medulloblastoma [9] and GBM [34] and is inhibited by GSI in a dose-dependent manner [7] in GBM CSCs. These findings were obtained by immunostaining-related approaches. Herein, an MS-based method was used to confirm the impact of the drug on NESTIN expression in GBM CSCs.

Two peptides from NESTIN were chosen according to the peptide selection criteria described in the experimental section. Table 2 shows the parent and fragment ion masses for the target peptides and heavy standard peptides. The most intense ions were selected for monitoring. Supporting Information 5 shows the MS/MS spectra used for the selection of the transitions. A total of four transitions were monitored for light and heavy GPPAPAPEVEELAR, and two transitions for light and heavy SLETEILESLK. Supporting Information 6 shows representative transitions for these

Table 2. Summary of the target peptides information and the transitions used for MRM analysis of Nestin

Peptide	Sequence	Label type	Charge	Parent ion	Product ion
Pep-1	SLETEILES�K	Unlabeled	2+	631.4	173 201
	SLETEILES�K*	Isotope-labeled	2+	635.1	173 201
Pep-2	GPPAPAPEVEELAR	Unlabeled	2+	716.9	127 155 252
					323
	GPPAPAPEVEELAR*	Isotope-labeled	2+	721.7	127 155 252 323

K* = Lys(¹³C₆, ¹⁵N₂); R* = Arg(¹³C₆, ¹⁵N₄).

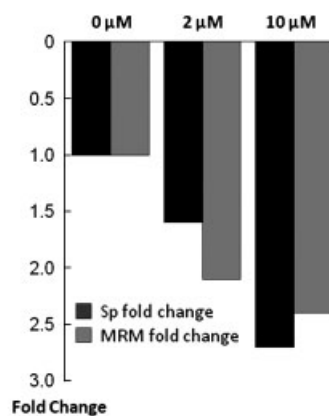
peptides in 0, 2, and 10 μM GSI-treated samples, while Supporting Information 7 shows all of the measured transitions for light and heavy SLETEILES�K. As expected, all transitions from each targeted peptide and its corresponding heavy standard were eluted at the same time.

The dose-dependent results from label-free data and the MRM data are shown in Fig. 4. Basically, the differential expression of NESTIN from the MRM results was consistent with the label-free quantitation data. As demonstrated by both of these methods, NESTIN exhibited reduced expression level along with increased GSI dosage. The expression level of NESTIN was reduced by ~1.3–3.5-fold when treating GBM CSCs with 2 and 10 μM GSI. This is in line with our previous report that a reduced mRNA NESTIN expression is detected from ~1.5 to 4-fold after treating GBM CSCs with GSI at 2 and 10 μM [7].

3.6 Altered signaling events upon GSI treatment

Based on the knowledge obtained from a combination of literature mining and data mining, candidate proteins listed in Table 1 and three proteins out of this table that have been verified (APC5, GFAP, and ENOG) were integrated to construct a putative altered signaling network after treating GBM CSCs with GSI, as depicted in Fig. 5. In addition, another three proteins were also imported: Thioredoxin (THIO/Trx), T-complex protein 1 subunit eta (TCPH/CCT7) and Hexokinase-1(HKX1). The first two proteins successfully passed checkpoint-2 with a *p*-value < 0.05 in 0 versus 10 μM and 0 versus 50 μM treatments although they are not differentially expressed after 2 μM treatment. The third protein passed checkpoint-1 but did not pass checkpoint-2 and it shows decreased expression upon 10 and 50 μM treatment. The correlation between these proteins and their targeted functions are listed in Table 3.

The majority of altered signaling events depicted in this figure are mediated through the Notch signaling cascade. Upon blockade of the Notch pathway, proliferation of CSCs



Sp Data	GSI-0μM		GSI-2μM		GSI-10μM	
	Mean	CV	Mean	CV	Mean	CV
Nestin	48	13%	30	17%	18	4%

Figure 4. Summary of the comparison between the fold change results obtained from label-free quantification by LTQ and MRM quantification by QqQ. The y-axis in the upper bar chart represents a ratio of fold changes by dividing the response from each treatment by control. The response of control is normalized to “1”. The lower panel provides the mean and CV of the spectral counts information for Nestin in each sample. “Spectral Counts” is abbreviated as “Sp”.

is selectively reduced [7], which is supported by our finding of decreased expression level of four key proteins: NESTIN, ENOG, PCNA, and proliferation-associated protein 2G4 (PA2G4). Also, differentiation is induced [7] which can be indicated by the elevated expression levels of two marker proteins for differentiated neural cells: GFAP and tubulin β-3 chain (TBB3). Previous studies in multiple myeloma report that activation of Notch signaling inhibits apoptosis while inhibition of Notch induces apoptosis [35, 36]. We also have demonstrated that Notch inhibition by GSI induces apoptosis in medulloblastoma and GBM [7, 9, 12]. Our results are in line with this where the blockade of Notch

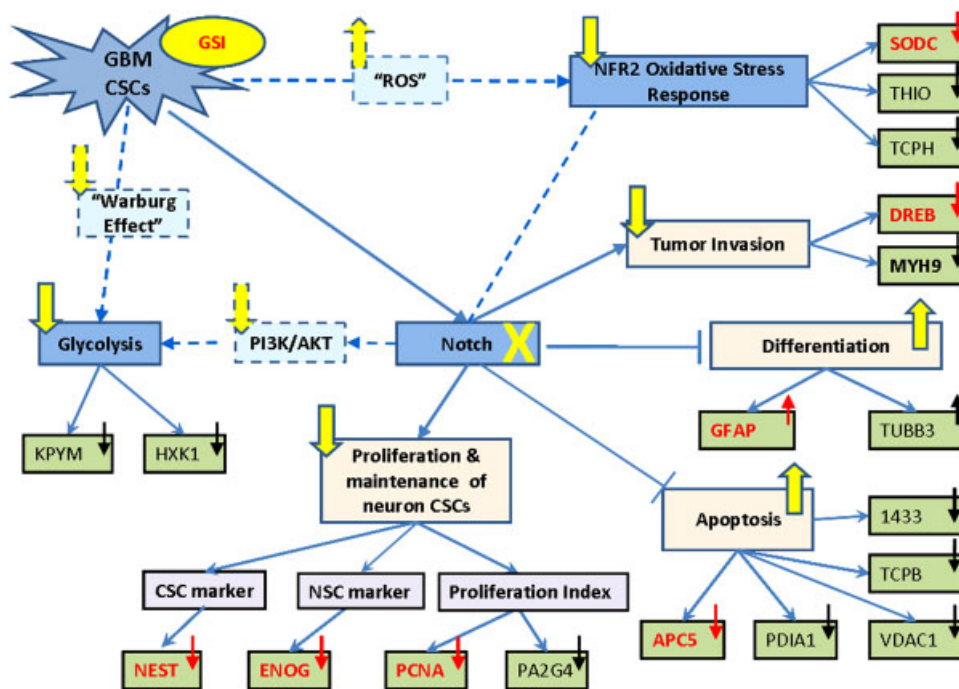


Figure 5. Putative altered signaling events occurring upon treatment of GSI. From our current understanding: GBM CSCs signals Notch pathway leading to a constitutive activation. Sequentially, Notch signaling activates the proliferation and maintenance of the undifferentiated CSCs, while suppressing apoptosis and differentiation. Treating GBM CSCs with GSI impairs Notch signaling and therefore reverses the above effects, which is suggested from our results and previous publications. In addition, NFR2-mediated oxidative response and glycolysis are also suggested to be down-regulated from our results possibly due to their crosstalk with Notch signaling. Solid line/arrow indicates a conclusion that is drawn based on our results and/or from previous publications with higher confidence. Dashed line/arrow indicates our hypothesis. The direction of an arrow placed in each node represents up/down-regulation of this protein or signaling pathway, while the arrow used to link adjacent nodes represents activation and the blunt end represents inhibition. Blue arrow/line indicates the native state of GBM CSCs while yellow arrow/line indicates the alterations occurring upon GSI treatment. Black arrow indicates the up/down-regulation detected in this study while red arrow indicates the ones that have been further validated by orthogonal approaches in our experiment.

activates apoptosis in GBM CSCs. This is supported by the detection of a reduced expression level of APC5, protein disulfide-isomerase (PDI1), voltage-dependent anion-selective channel protein 1 (VDAC1), TCPB and 1433 proteins, all of which have been reported to be negatively correlated with apoptosis [31, 37–44]. In addition, decreased tumor invasion capability is inferred and supported by the detection of reduced expression of DREB and myosin-9 (MYH9) which are identified to be positively correlated with metastasis [45–47].

Another signaling cascade we speculate to be down-regulated is NFR2-mediated oxidative response which contributes to cellular protection against oxidative insults and chemical carcinogens [48]. The decreased expression levels of its downstream transcriptional gene products, such as anti-oxidant proteins, SODC and THIO, and a molecular chaperone protein, TCPH, imply that this cellular defense system against ROS has been attenuated [32, 49–51]. As aforementioned, treating GBM CSCs with GSI tends to abrogate the stem cell properties [7]. It is thus reasonable to infer that the decreased oxidative defense capability is also

correlated with a phenotype transformation from CSCs towards non-tumorigenic cells. This hypothesis is in light of the recent significant discoveries that subsets of CSCs in some tumors contain an enhanced defense system compared to non-tumorigenic progeny suggested by lower ROS levels [52–53]. However, it is uncertain at this point that the down-regulation of NFR2-mediated oxidative response is attributed to the direct impact from the impaired γ -secretase activity or via its newly proposed crosstalk mechanism with Notch signaling [54].

In addition, the glucose metabolism pathway glycolysis is also suggested to be down-regulated. Most cancer cells rely on anaerobic metabolism even with an abundance of oxygen rather than mitochondrial oxidative phosphorylation for normal differentiated cells and the glycolytic rate is increased to compensate for the less efficient production of ATP, a phenomenon referred to as the “Warburg effect” [55]. The expression of two out of three rate-limiting key enzymes in glycolysis: pyruvate kinase isozymes M1/M2 (KPYM) and HKX1, were found to be decreased from our label free quantitative data, which may imply a decrease of

Table 3. Correlation between the proteins used for constructing the altered signaling network and their targeted functions

Functions	Protein	Correlation	Reference
Proliferation	PCNA	+	[23, 24]
	NEST	+	[7, 9, 27, 32, 33]
	PA2G4	+	[13]
Differentiation	ENOG	+	[25, 26]
	TBB3	+	[27]
Apoptosis	GFAP	+	[27]
	APC5	–	[30]
Tumor invasion	PDIA1	–	[39, 40]
	VDAC1	–	[41, 42]
	TCPB	–	[43]
	1433-serise	–	[44]– [46]
Oxidative response	DREB	+	[36]
	MYH9	+	[47, 48]
Glycolysis	SODC	+	[31]
	THIO	+	[50, 51]
Glycolysis	TCPH	+	[52]
	KPYM	+	[59]
	HKX1	+	[59]

“+” indicates positive association and “–” indicates negative association, which are learned from the previous literature publications as listed in the “Reference” column.

glycolytic rate after blockade of Notch signaling. This inference regarding the relationship between Notch pathway and glycolysis could be supported by previous investigations showing that Notch signals promote glucose metabolism mediated by the PI3K/AKT pathway [56] and our previous finding showing that Notch pathway blockade by GSI reduces AKT phosphorylation in medulloblastoma and GBM [7, 9, 12]. Another study of Pre-T cells has also shown that the withdrawal of Notch signaling reduced AKT phosphorylation and decreased the glycolytic rate [57]. Moreover, the PI3K/AKT pathway has been shown to stimulate aerobic glycolysis in cancer cells [58] and directly enhance glucose capture by HKX1 [59]. Therefore, we hypothesize that the blockade of Notch Pathway upon GSI treatment decreases PI3K/AKT signaling which further suppresses glycolysis. Another explanation to the hypothetical decreased glucose metabolism is that GSI treatment may induce a mechanistic switch back to aerobic metabolism so that the accelerated production of pyruvate is not needed; hence the glucose metabolism is down-regulated. There is no available evidence indicating that the impaired γ -secretase activity has a direct impact on the suppression of glycolysis.

Another interesting link between NFR2 oxidative response and glycolysis is the level of ROS. The generation of ROS has been postulated to be increased as the glycolytic rate is reduced [59] and also as the oxidative defense decreased in non-tumorigenic cells compared to CSCs [53]. We have discussed above our inferences that the treatment of GSI drives a transformation towards non-tumorigenic cells, suppresses the cell defense capability and down-regulates aerobic glycolysis. Thus, it is also reasonable to

infer that the level of ROS is increased after the treatment in GBM CSCs, although it is uncertain about the alteration mechanism of mitochondrial oxidative phosphorylation which is the major cellular source of ROS production.

3.7 IPA

To gain additional insight from our data, an alternative data mining tool was utilized to construct significantly affected canonical pathways upon GSI treatment by IPA. Glycolysis, NFR2-mediated oxidative stress response and PI3K/AKT signaling are captured as the most significant canonical pathways which provide another piece of evidence to support our hypothesis from a bioinformatics perspective. Other important signaling pathways are also shown including VEGF signaling, cell cycle, and hypoxia signaling, etc. This may be attributed to the demonstrated crosstalk between Notch signaling and these pathways [60, 61] or GSI may also have direct impact on these pathways. The detailed pathway lists can be found in Supporting Information 8. One needs to be careful about the interpretation of the level of the significance between the treatments. The length of the bar indicates a level of association that is by no means indicative of either up or down regulation. Also, most of the pathways appear to be increasingly significant in the third treatment (50 μ M GSI). This may be because more proteins are differentially expressed between the treatment and the control as the dosage increases. Thus, the increased number of imported proteins may affect the outcome of the statistic algorithm (Fisher's exact *t*-test) adopted by IPA for the calculation of significance by inducing a smaller *p*-value.

4 Concluding remarks

In summary, this work adopts a label-free quantitative global proteomic approach together with Immunoassay and MRM assays to conduct a dose-dependent investigation on the proteome alterations upon the treatment of GSI in GBM CSCs. It demonstrates a work-flow from global discovery, candidate prioritization to verification phase which could be applied to other studies as well. By coupling our results with previous literature reports from our group and others, a putative signaling network consisting of 21 candidate proteins with 7 being verified is generated to reflect our inference of the underlying molecular alterations upon GSI treatment. The downstream effects resulting from the blockade of Notch signaling are suggested to include a reduced proliferative potential, an increased differentiation and an elevated apoptotic activity, leading to a phenotype transformation towards non-tumorigenic cells. Novel involvement of the down-regulated NFR2-mediated oxidative stress response and glycolysis are implied as a consequence of GSI treatment, possibly due to their crosstalk to Notch signaling. These findings regarding the

alterations occurring on the proteome level and the signaling/metabolic pathway level provide enriched information that could broaden our current knowledge about drug mechanism, contributing to the identification of novel drug targets to develop better therapies for treating this dismal disease.

This work was funded under the National Institute of Health Grants R01 49500 (D.M.L.) and R21 CA134623 (D.M.L.) S.P. acknowledges grant support from the NIDDK, Molecular Phenotyping Core, Michigan Nutrition and Obesity Center (DK089503) and the Doris Duke Foundation. The authors acknowledge grant support to Dr. Fan from Accelerate Brain Cancer Cure Project Award, American Brain Tumor Association Translational Grant, and Voices Against Brain Cancer Research Grant.

The authors have declared no conflict of interest.

5 References

- [1] Stupp, R., Mason, W. P., van den Bent, M. J., Weller, M. et al., Radiotherapy plus concomitant and adjuvant temozolomide for glioblastoma. *N. Engl. J. Med.* 2005, **352**, 987–996.
- [2] Vescovi, A. L., Galli, R., Reynolds, B. A., Brain tumour stem cells. *Nat. Rev. Cancer* 2006, **6**, 425–436.
- [3] Read, T. A., Fogarty, M. P., Markant, S. L., McLendon, R. E. et al., Identification of CD15 as a marker for tumor-propagating cells in a mouse model of medulloblastoma. *Cancer Cell* 2009, **15**, 135–147.
- [4] Ward, R. J., Lee, L., Graham, K., Satkunendran, T. et al., Multipotent CD15+ cancer stem cells in patched-1-deficient mouse medulloblastoma. *Cancer Res.* 2009, **69**, 4682–4690.
- [5] Son, M. J., Woolard, K., Nam, D. H., Lee, J., Fine, H. A., SSEA-1 is an enrichment marker for tumor-initiating cells in human glioblastoma. *Cell Stem Cell* 2009, **4**, 440–452.
- [6] Gilbert, C. A., Ross, A. H., Cancer stem cells: cell culture, markers, and targets for new therapies. *J. Cell Biochem.* 2009, **108**, 1031–1038.
- [7] Fan, X., Khaki, L., Zhu, T. S., Soules, M. E. et al., NOTCH pathway blockade depletes CD133-positive glioblastoma cells and inhibits growth of tumor neurospheres and xenografts. *Stem Cells* 2010, **28**, 5–16.
- [8] Stockhausen, M. T., Kristoffersen, K., Poulsen, H. S., The functional role of Notch signaling in human gliomas. *Neuro. Oncol.* 2010, **12**, 199–211.
- [9] Fan, X., Matsui, W., Khaki, L., Stearns, D. et al., Notch pathway inhibition depletes stem-like cells and blocks engraftment in embryonal brain tumors. *Cancer Res.* 2006, **66**, 7445–7452.
- [10] Wang, J., Wakeman, T. P., Lathia, J. D., Hjelmeland, A. B. et al., Notch promotes radioresistance of glioma stem cells. *Stem Cells* 2010, **28**, 17–28.
- [11] Chiba, S., Notch signaling in stem cell systems. *Stem Cells* 2006, **24**, 2437–2447.
- [12] Fan, X., Eberhart, C. G., Medulloblastoma stem cells. *J. Clin. Oncol.* 2008, **26**, 2821–2827.
- [13] Steiniger, S. C., Coppinger, J. A., Kruger, J. A., Yates 3rd, J., Janda, K. D., Quantitative mass spectrometry identifies drug targets in cancer stem cell-containing side population. *Stem Cells* 2008, **26**, 3037–3046.
- [14] Bendall, S. C., Hughes, C., Campbell, J. L., Stewart, M. H. et al., An enhanced mass spectrometry approach reveals human embryonic stem cell growth factors in culture. *Mol. Cell. Proteomics* 2009, **8**, 421–432.
- [15] Williamson, A. J., Smith, D. L., Blinco, D., Unwin, R. D. et al., Quantitative proteomics analysis demonstrates post-transcriptional regulation of embryonic stem cell differentiation to hematopoiesis. *Mol. Cell. Proteomics* 2008, **7**, 459–472.
- [16] Dai, L., Li, C., Shedden, K. A., Lee, C. J. et al., Quantitative proteomic profiling studies of pancreatic cancer stem cells. *J. Proteome Res.* 2010, **9**, 3394–3402.
- [17] Kitteringham, N. R., Jenkins, R. E., Lane, C. S., Elliott, V. L., Park, B. K., Multiple reaction monitoring for quantitative biomarker analysis in proteomics and metabolomics. *J. Chromatogr. B Analyt. Technol. Biomed. Life Sci.* 2009, **877**, 1229–1239.
- [18] Prakash, A., Tomazela, D. M., Frewen, B., Maclean, B. et al., Expediting the development of targeted SRM assays: using data from shotgun proteomics to automate method development. *J. Proteome Res.* 2009, **8**, 2733–2739.
- [19] Lopez, M. F., Kuppasamy, R., Sarracino, D. A., Prakash, A. et al., Mass spectrometric discovery and selective reaction monitoring (SRM) of putative protein biomarker candidates in first trimester Trisomy 21 maternal serum. *J. Proteome Res.* 2011, **10**, 133–142.
- [20] Galli, R., Binda, E., Orfanelli, U., Cipelletti, B. et al., Isolation and characterization of tumorigenic, stem-like neural precursors from human glioblastoma. *Cancer Res.* 2004, **64**, 7011–7021.
- [21] Keller, A., Nesvizhskii, A. I., Kolker, E., Aebersold, R., Empirical statistical model to estimate the accuracy of peptide identifications made by MS/MS and database search. *Anal. Chem.* 2002, **74**, 5383–5392.
- [22] Dai, L., Li, C., Shedden, K. A., Misek, D. E., Lubman, D. M., Comparative proteomic study of two closely related ovarian endometrioid adenocarcinoma cell lines using cIEF fractionation and pathway analysis. *Electrophoresis* 2009, **30**, 1119–1131.
- [23] Liu, J. W., Jiao, N. Z., Hong, H. S., Luo, T. W., Cai, H. Y., Proliferating cell nuclear antigen (PCNA) as a marker of cell proliferation in the marine dinoflagellate *Prorocentrum donghaiense* Lu and the green alga *Dunaliella salina* Teodoresco. *J. Appl. Phycol.* 2005, **17**, 323–330.
- [24] Ma, X. B., Jia, X. S., Liu, Y. L., Wang, L. L. et al., Expression and role of Notch signalling in the regeneration of rat tracheal epithelium. *Cell Prolif.* 2009, **42**, 15–28.
- [25] Mitchell, K. E., Weiss, M. L., Mitchell, B. M., Martin, P. et al., Matrix cells from Wharton's jelly form neurons and glia. *Stem Cells* 2003, **21**, 50–60.

- [26] Prestegarden, L., Svendsen, A., Wang, J., Sleire, L. et al., Glioma cell populations grouped by different cell type markers drive brain tumor growth. *Cancer Res.* 2010, *70*, 4274–4279.
- [27] Rebetz, J., Tian, D., Persson, A., Widegren, B. et al., Glial progenitor-like phenotype in low-grade glioma and enhanced CD133-expression and neuronal lineage differentiation potential in high-grade glioma. *PLoS One* 2008, *3*, e1936.
- [28] Singh, S. K., Clarke, I. D., Terasaki, M., Bonn, V. E. et al., Identification of a cancer stem cell in human brain tumors. *Cancer Res.* 2003, *63*, 5821–5828.
- [29] Park, K. H., Choi, S. E., Eom, M., Kang, Y., Downregulation of the anaphase-promoting complex (APC)7 in invasive ductal carcinomas of the breast and its clinicopathologic relationships. *Breast Cancer Res.* 2005, *7*, R238–R247.
- [30] Bentley, A. M., Williams, B. C., Goldberg, M. L., Andres, A. J., Phenotypic characterization of *Drosophila* *ida* mutants: defining the role of APC5 in cell cycle progression. *J. Cell Sci.* 2002, *115*, 949–961.
- [31] Wang, Q., Moyret-Lalle, C., Couzon, F., Surbiguet-Clippe, C. et al., Alterations of anaphase-promoting complex genes in human colon cancer cells. *Oncogene* 2003, *22*, 1486–1490.
- [32] Haapasalo, H., Kylaniemi, M., Paunul, N., Kinnula, V. L., Soini, Y., Expression of antioxidant enzymes in astrocytic brain tumors. *Brain Pathol.* 2003, *13*, 155–164.
- [33] Hemmati, H. D., Nakano, I., Lazareff, J. A., Masterman-Smith, M. et al., Cancerous stem cells can arise from pediatric brain tumors. *Proc. Natl. Acad. Sci. USA* 2003, *100*, 15178–15183.
- [34] Shih, A. H., Holland, E. C., Notch signaling enhances nestin expression in gliomas. *Neoplasia* 2006, *8*, 1072–1082.
- [35] Nefedova, Y., Sullivan, D. M., Bolick, S. C., Dalton, W. S., Gabilovich, D. I., Inhibition of Notch signaling induces apoptosis of myeloma cells and enhances sensitivity to chemotherapy. *Blood* 2008, *111*, 2220–2229.
- [36] Jia, X. X., Lu, Z. Z., Wang, H., Duan, H. F. et al., Suppressive effect of Notch signal activation on apoptosis of multiple myeloma cells. *Zhongguo Shi Yan Xue Ye Xue Za Zhi* 2004, *12*, 335–339.
- [37] Lovat, P. E., Corazzari, M., Armstrong, J. L., Martin, S. et al., Increasing melanoma cell death using inhibitors of protein disulfide isomerases to abrogate survival responses to endoplasmic reticulum stress. *Cancer Res.* 2008, *68*, 5363–5369.
- [38] Cui, Y., Zhu, H., Zhu, Y., Guo, X. et al., Proteomic analysis of testis biopsies in men treated with injectable testosterone undecanoate alone or in combination with oral levonorgestrel as potential male contraceptive. *J. Proteome Res.* 2008, *7*, 3984–3993.
- [39] Pathil, A., Armeanu, S., Venturelli, S., Mascagni, P. et al., HDAC inhibitor treatment of hepatoma cells induces both TRAIL-independent apoptosis and restoration of sensitivity to TRAIL. *Hepatology* 2006, *43*, 425–434.
- [40] Singh, T. R., Shankar, S., Srivastava, R. K., HDAC inhibitors enhance the apoptosis-inducing potential of TRAIL in breast carcinoma. *Oncogene* 2005, *24*, 4609–4623.
- [41] Zhao, Z. L., Li, Q. F., Zheng, Y. B., Chen, L. Y. et al., The aberrant expressions of nuclear matrix proteins during the apoptosis of human osteosarcoma cells. *Anat. Rec. (Hoboken)* 2010, *293*, 813–820.
- [42] Xing, H., Zhang, S., Weinheimer, C., Kovacs, A., Muslin, A. J., 14-3-3 proteins block apoptosis and differentially regulate MAPK cascades. *Embo J.* 2000, *19*, 349–358.
- [43] Rosenquist, M., 14-3-3 proteins in apoptosis. *Braz. J. Med. Biol. Res.* 2003, *36*, 403–408.
- [44] Cao, W., Yang, X., Zhou, J., Teng, Z. et al., Targeting 14-3-3 protein, difopein induces apoptosis of human glioma cells and suppresses tumor growth in mice. *Apoptosis* 2010, *15*, 230–241.
- [45] Perez-Martinez, M., Gordon-Alonso, M., Cabrero, J. R., Barrero-Villar, M. et al., F-actin-binding protein drebrin regulates CXCR4 recruitment to the immune synapse. *J. Cell Sci.* 2010, *123*, 1160–1170.
- [46] Betapudi, V., Myosin II motor proteins with different functions determine the fate of lamellipodia extension during cell spreading. *PLoS One* 2010, *5*, e8560.
- [47] Medjkane, S., Perez-Sanchez, C., Gaggioli, C., Sahai, E., Treisman, R., Myocardin-related transcription factors and SRF are required for cytoskeletal dynamics and experimental metastasis. *Nat. Cell Biol.* 2009, *11*, 257–268.
- [48] Cho, H. Y., Reddy, S. P., Debiase, A., Yamamoto, M., Kleeberger, S. R., Gene expression profiling of NRF2-mediated protection against oxidative injury. *Free Radic. Biol. Med.* 2005, *38*, 325–343.
- [49] Gomez-Pastor, R., Perez-Torrado, R., Cabisco, E., Ros, J., Matallana, E., Reduction of oxidative cellular damage by overexpression of the thioredoxin TRX2 gene improves yield and quality of wine yeast dry active biomass. *Microb. Cell Fact.* 2010, *9*, 9.
- [50] Ronkainen, H., Vaarala, M. H., Kauppila, S., Soini, Y. et al., Increased BTB-Kelch type substrate adaptor protein immunoreactivity associates with advanced stage and poor differentiation in renal cell carcinoma. *Oncol. Rep.* 2009, *21*, 1519–1523.
- [51] Go, Y. M., Craig, S. E., Orr, M., Gernert, K. M., Jones, D. P., Gene and protein responses of human monocytes to extracellular cysteine redox potential. *Toxicol. Sci.* 2009, *112*, 354–362.
- [52] Kai, K., Arima, Y., Kamiya, T., Saya, H., Breast cancer stem cells. *Breast Cancer* 2010, *17*, 80–85.
- [53] Diehn, M., Cho, R. W., Lobo, N. A., Kalisky, T. et al., Association of reactive oxygen species levels and radioresistance in cancer stem cells. *Nature* 2009, *458*, 780–783.
- [54] Wakabayashi, N., Shin, S., Slocum, S. L., Agoston, E. S. et al., Regulation of notch1 signaling by nrf2: implications for tissue regeneration. *Sci. Signal* 2010, *3*, ra52.
- [55] Warburg, O., On the origin of cancer cells. *Science* 1956, *123*, 309–314.
- [56] Palomero, T., Dominguez, M., Ferrando, A. A., The role of the PTEN/AKT Pathway in NOTCH1-induced leukemia. *Cell Cycle* 2008, *7*, 965–970.

- [57] Ciofani, M., Zuniga-Pflucker, J. C., Notch promotes survival of pre-T cells at the beta-selection checkpoint by regulating cellular metabolism. *Nat. Immunol.* 2005, *6*, 881–888.
- [58] Elstrom, R. L., Bauer, D. E., Buzzai, M., Karnauskas, R. et al., Akt stimulates aerobic glycolysis in cancer cells. *Cancer Res.* 2004, *64*, 3892–3899.
- [59] Vander Heiden, M. G., Cantley, L. C., Thompson, C. B., Understanding the Warburg effect: the metabolic requirements of cell proliferation. *Science* 2009, *324*, 1029–1033.
- [60] Kanamori, M., Kawaguchi, T., Nigro, J. M., Feuerstein, B. G. et al., Contribution of Notch signaling activation to human glioblastoma multiforme. *J. Neurosurg.* 2007, *106*, 417–427.
- [61] Lee, S. H., Kim, M. H., Han, H. J., Arachidonic acid potentiates hypoxia-induced VEGF expression in mouse embryonic stem cells: involvement of Notch, Wnt, and HIF-1alpha. *Am. J. Physiol. Cell Physiol.* 2009, *297*, C207–C216.